Neuron, Vol. 45, 447–457, February 3, 2005, Copyright ©2005 by Elsevier Inc. DOI 10.1016/j.neuron.2004.12.042

Positive Feedback in a Brainstem Tactile Sensorimotor Loop

Quoc-Thang Nguyen[1] and David Kleinfeld[1,2,3,*]
[1]Department of Physics
[2]Center for Theoretical Biological Physics
[3]Neurosciences Graduate Program
University of California at San Diego
La Jolla, California 92093

Summary

The trigeminal loop in the brainstem comprises the innermost level of sensorimotor feedback in the rat vibrissa system. Anatomy suggests that this loop relays tactile information from the vibrissae to the motoneurons that control vibrissa movement. We demonstrate, using in vitro and in vivo recordings, that the trigeminal loop consists of excitatory pathways from vibrissa sensory inputs to vibrissa motoneurons in the facial nucleus. We further show that the trigeminal loop implements a rapidly depressing reflex that provides positive sensory feedback to the vibrissa musculature during simulated whisking and contact. On the basis of these findings, we propose that the trigeminal loop provides an enhancement of vibrissa muscle tone upon contact during active touch.

Introduction

Active touch is a commonly observed behavior that animals use to explore their surrounding environment, discern shapes, and enhance texture detection (Gibson, 1962; Gamzu and Ahissar, 2001). The resulting haptic sensations are used in a recurrent fashion to finely tune the position or the motion of tactile sensors (Voisin et al., 2002). The transformation of sensory inputs into modulatory motor outputs during active touch is performed by sensorimotor feedback loops whose functional properties are largely unknown.

In the rat vibrissa somatosensory system, the vibrissa trigeminal loop in the brainstem is the first circuit in which vibrissa sensorimotor integration occurs (Kis et al., 2004; Kleinfeld et al., 1999) (Figure 1A). In this loop, signals from vibrissae ascend the infraorbital branch (IoN) of the trigeminal nerve (V-th nerve) to primary sensory neurons in the trigeminal ganglion (TG). These cells project to second order sensory neurons in the trigeminal nuclear (TN) complex, which consists of the principalis nucleus (PrV) and the spinal trigeminal nuclei pars interpolaris (SpVi), pars oralis (SpVo), and pars caudalis (SpVc). Subcortical whisking centers, which include a brainstem whisking central pattern generator (Gao et al., 2001; Hattox et al., 2003), send motor commands to vibrissa motoneurons in the facial nucleus (FN). These cells project to vibrissa muscles via the facial nerve (VII-th nerve). Intrinsic muscles, which are responsible for vibrissa protraction, are innervated by the buccolabialis (BL) branch of the facial nerve, while the extrinsic muscle levator labii superioris, which retracts the mystacial pad during exploratory whisking (Berg and Kleinfeld, 2003), is innervated by the zygomaticoorbitalis branch of the VII-th nerve (Dörfl, 1982). The trigeminal loop is closed by direct projection from PrV, SpVi, and SpVc to the facial nucleus (Erzurumlu and Killackey, 1979; Hattox et al., 2002) and indirect pathways within the brainstem via the pontomedullary reticular formation (RF) (Dauvergne et al., 2001; Zerari-Mailly et al., 2001). Higher-order loops involve collicular, cerebellar, and dorsal thalamic areas (Kleinfeld et al., 1999) (Figure 1A).

It is well established that the sensory branch of the vibrissa trigeminal loop, i.e., TG to TN, is excitatory (Guido et al., 2001; Lo et al., 1999; Minnery and Simons, 2003; Onodera et al., 2000; Sosnik et al., 2001; Zucker and Welker, 1969). Yet the net sign and delay time of potential feedback in the greater loop are unknown, although there are limited GABAergic and glycinergic projections from the spinal trigeminal nuclei pars oralis and interpolaris to the facial nucleus (Li et al., 1997). Further, there are no proprioceptors in the mystacial musculature (Rice et al., 1997) and no reported monosynaptic connections between trigeminal ganglion cells and vibrissa motoneurons. Here, we address the issues of feedback in the trigeminal loop through the use of in vitro and in vivo preparations. In the former approach, we developed a 1000 to 1200 μm thick horizontal brainstem slice from newborn (P7 to P9) and older (P12 to P15) rats that contains the sensory and motor nuclei of the vibrissa trigeminal loop as well as the trigeminal nerve and ganglion (Figure 1B). We stimulated the sensory nerve and recorded intracellular potentials from vibrissa motoneurons. In the latter approach, we used adult anesthetized animals and placed electromyogram (EMG) electrodes inside the ipsilateral mystacial pad to record intrinsic muscle activity and in the levator labii superioris muscle to record the activity of a single extrinsic muscle (Berg and Kleinfeld, 2003; Dörfl, 1982; Wineski, 1983).

Results

Brainstem Slice

Suprathreshold stimulation of the IoN ipsilateral to the motoneurons elicited delayed, subthreshold excitatory postsynaptic potentials (EPSPs) (Figure 1C) in 50% of the motoneurons that we recorded (P7 to P9). The responses exhibited peaks with latencies that extended up to 1 s after stimulus onset (Figure 1C). While the responses varied from trial to trial, the earliest EPSPs added in phase upon averaging across trials (Figure 1C, inset).

Dissection of the trigeminal nerve to isolate the IoN is much more time-intensive and problematic in older, whisking animals than it is in young animals. Thus the trigeminal nerve was left intact for the preparation of slices from P12 to P15 animals. Nonetheless, stimulation of the entire trigeminal nerve led to essentially

*Correspondence: dk@physics.ucsd.edu

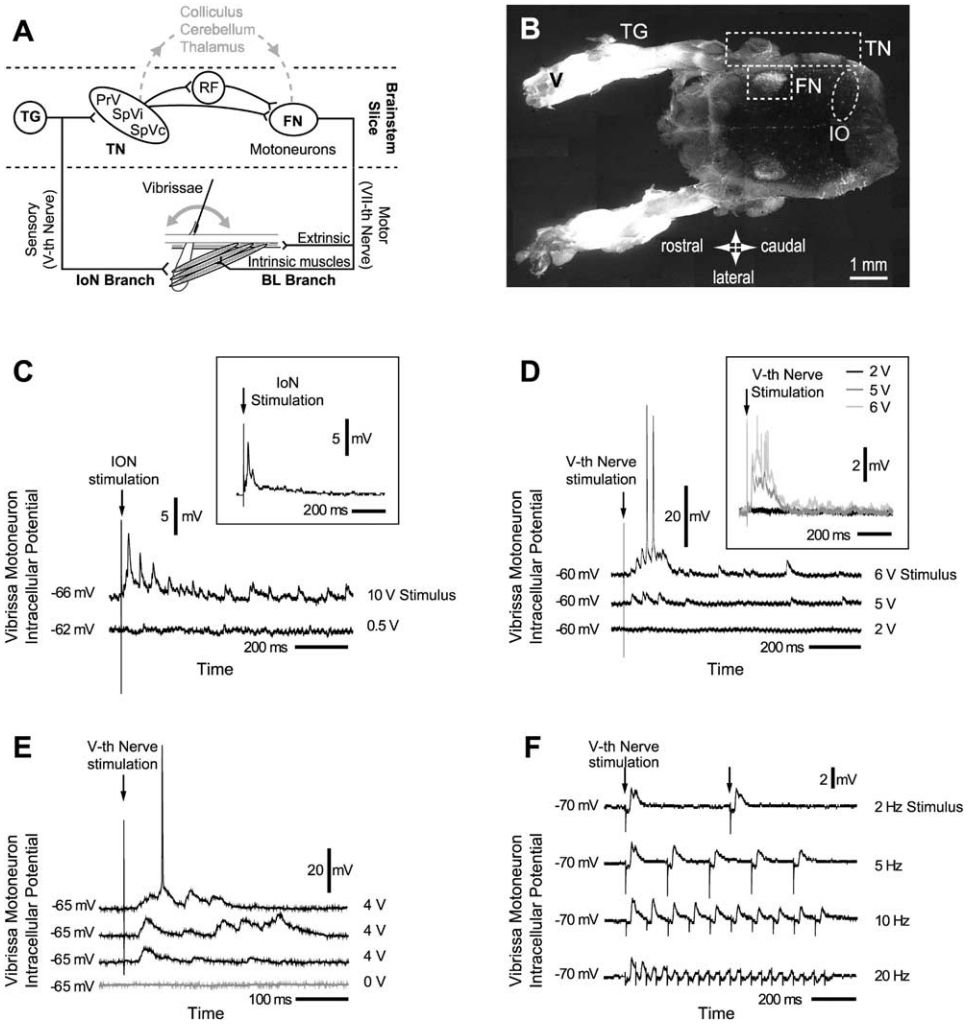

Figure 1. The Vibrissa Trigeminal Loop and Basic Response

(A) The vibrissa trigeminal loop in the rat brainstem. The gray dashed line indicates supratrigeminal sensorimotor loops. The black dashed lines outline the boundaries of the slice preparation. BL, buccolabialis branch of facial nerve; FN, facial nucleus; IoN, infraorbital branch of trigeminal nerve; PrV, principalis nucleus; RF, pontomedullary reticular formation; SpVc, spinal trigeminal nucleus pars caudalis; SpVi, spinal trigeminal nucleus pars interpolaris; TG, trigeminal ganglion; TN, trigeminal nuclear complex. (B) Brainstem slice from a P12 rat. The dashed box labeled FN outlines vibrissa motoneurons retrogradely labeled by Evans Blue. The dashed box labeled TN surrounds the trigeminal nuclear sensory complex. IO, inferior olive; V, trigeminal nerve. (C) EPSPs in vibrissa motoneurons following stimulation of the ipsilateral IoN in a slice from a P9 animal. Upper trace, response obtained with a 10 V IoN stimulation; lower trace, control with subthreshold 0.5 V stimulation; inset, average of 20 responses at 10 V stimulation. (D) EPSPs following stimulation of the ipsilateral trigeminal nerve in a slice from a P12 animal. Upper trace, response obtained with suprathreshold stimulation for spikes; lower trace, control with 2 V stimulation; inset, average of 20 responses with increasing stimulation voltage. (E) Trial-to-trial variability of EPSPs following stimulation of the ipsilateral trigeminal nerve in a slice from a P12 animal. (F) Postsynaptic depression of the motoneuron response. Traces are averages of ten trials.

identical responses to those for which the IoN was stimulated (Figures 1D and 1E; P12 to P15). The EPSPs had a stable stimulation threshold (Figures 1C and 1D) and, as in the case of motoneurons from newborns, occurred for up to 1 s after the stimulus onset (Figure 1D). Further, the stimulus could evoke one or several action potentials (15% of the neurons) when the stimulation voltage was increased above the threshold value (Figure 1D). As in the case with newborn animals, only the EPSPs that occurred earliest would add in phase across trials, and those EPSPs became gradually larger as the stimulation voltage was increased (n = 9 neurons) (Figure 1D, inset). Lastly, the response was observed to depress after successive periodic stimuli for frequencies above 2 Hz (n = 5 neurons) (Figure 1F). By 9 Hz, the mean frequency for exploratory whisking (Berg and Kleinfeld, 2003), the steady-state amplitude of the EPSPs was attenuated by ~40%.

As a control to verify that responses evoked by trigeminal nerve stimulation were not indiscriminately elicited throughout the slice, we recorded from neurons in the inferior olive, a structure that is not part of the vibrissa trigeminal loop. Neurons were selected on the basis of their location in the slice and the presence of

subthreshold oscillations and a prominent depolarization sag (Llinás and Yarom, 1981). In all neurons tested (n = 12), extracellular stimulation of the ipsilateral trigeminal nerve with voltage pulses as high as 30 V did not elicit a response (data not shown), unlike vibrissa motoneurons in the same slice.

The averaged EPSPs had maximal amplitudes that ranged from 0.5 to 12 mV and rise and decay times of ~2 ms and ~20 ms, respectively. The amplitude of averaged EPSPs did not change noticeably when motoneurons were hyperpolarized by up to 30 mV by the injection of negative current (n = 5 neurons) (Figure 2A), consistent with the known distal location of synaptic boutons on dendrites (Friauf, 1986). We observed that the latency of the earliest EPSP (Δt in Figure 2A) was distributed in two populations: Δt_1, with latencies between 5 and 15 ms, and Δt_2, a group with latencies > 15 ms (Figure 2B). There was no significant difference in the distributions of the latencies of the EPSPs between the P7 to P9 and P11 to P15 age groups (Table 1) and no significant correlation between the value of the latency and the corresponding amplitude (Figure 2C).

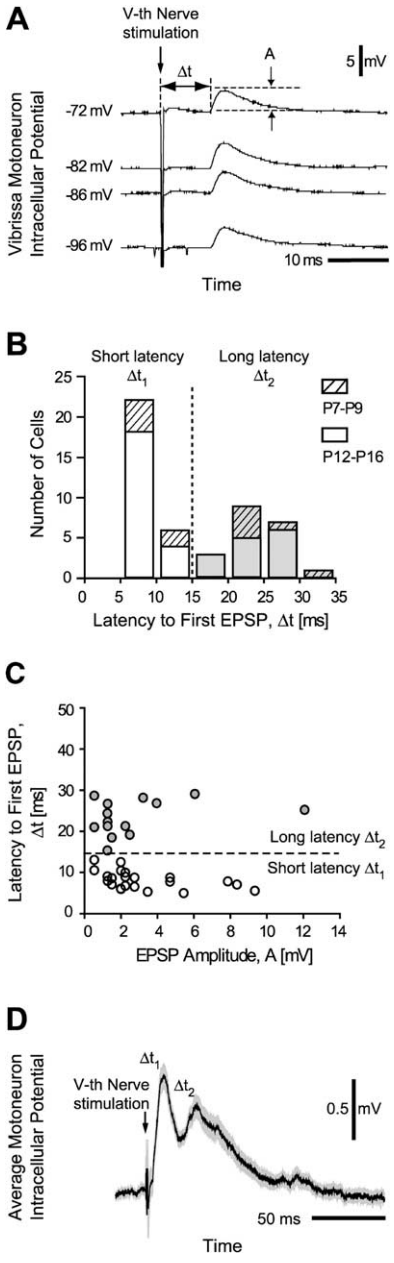

Figure 2. Nature of the Motoneuron EPSPs

(A) Averaged EPSPs (20 trials) at different membrane potentials. (B) Distribution of the latency to the first EPSP, Δt as defined in (A) (white bars, cluster denoted Δt_1; gray bars, cluster denoted Δt_2) in P7 to P9 (hatched) and P12 to P15 preparations (clear). (C) Distribution of the maximal amplitude, A (see [A]) versus EPSP latency in vibrissa motoneurons from P12 to P15 animals. (D) Trial and preparation averaged intracellular response to trigeminal nerve stimulation. The responses from ten trials each of 25 motoneurons from P10 to P15 animals were averaged together; mean, black trace; SEM, gray band.

Whole Animals

Our in vitro results imply that activation of vibrissa sensory inputs in vivo should result in a biphasic EMG response in the vibrissa musculature. To test this prediction, sensory inputs in the intact, anesthetized rat were stimulated by two methods: (1) direct electrical stimulation of the IoN sensory branch; and (2) electrical stimulation of the buccolabialis motor branch, to elicit forward motion of the vibrissae and the concomitant generation of vibrissa sensory signals (Brown and Waite, 1974; Szwed et al., 2003; Zucker and Welker, 1969). To ascertain the behavioral relevance of the sensorimotor feedback, we measured EMG response during rhythmic stimulation by two methods, the first being passive deflection of the vibrissae and the second, electrical stimulation of the buccolabialis motor branch to elicit rhythmic motion and contact of the vibrissae with an obstacle.

IoN Stimulation

The IoN was electrically stimulated with currents above a threshold value of 1–5 mA (Figure 3A) (Fanselow and Nicolelis, 1999). We observed an EMG response in the intrinsic muscles locked to stimulus onset, whose amplitude and duration varied greatly from trial to trial. A prompt response, which occurred in 52% of the trials (n = 200), was denoted as Δt_1, in analogy with the in vitro data (Figure 2B). The observed latency was 5.5 ± 0.5 ms (mean ± SD) in urethane-anesthetized animals (n = 4 rats, 200 trials; data not shown) and 6.3 ± 1.3 ms in ketamine-anesthetized animals (n = 4 rats; Figure 3C, upper panel). Under ketamine, the initial EMG response was followed by a more complex EMG response after a brief period of inactivity. The latency of this response, denoted Δt_2, had a minimum value of 12 ms and an average value of 20 ms (Figure 3D). Critically, the latency distributions of in vitro motoneuron EPSPs and in vivo muscle responses were essentially identical (cf. lower panels in Figures 2B and 3D; Table 1). The complex response was not observed with urethane (Evinger et al., 1993), and thus all subsequent experiments employed ketamine anesthesia.

The responses for the extrinsic muscle were comparable to those for the intrinsic muscles (200 trials, n = 4; Figures 3C and 3D, lower panels). In general, the

Table 1. Averaged Response Latencies

Brainstem Slice – Sensory Nerve Stimulation	Δt_1 (ms)[a]	Δt_2 (ms)[a]
Infraorbital branch stimulation (P7 to P9) Motoneuron EPSPs	9.0 ± 2.0 (6)[c]	26.3 ± 4.9 (6)
Vth nerve stimulation (P12 to P15) Motoneuron EPSPs	8.1 ± 2.2 (21)	25.0 ± 3.7 (10)
In Vivo – Sensory Nerve Stimulation[b]		
Infraorbital sensory branch stimulation Intrinsic muscle EMG	6.3 ± 1.2 (105)[d]	21.3 ± 4.8 (73)
Infraorbital sensory branch stimulation Extrinsic muscle EMG	5.5 ± 1.7 (127)	21.0 ± 4.7 (25)
In Vivo – Motor Nerve Stimulation[b]		
Buccolabialis motor branch stimulation Intrinsic muscle EMG	11.9 ± 1.5 (75)[d]	21.4 ± 6.7 (81)
Buccolabialis motor branch stimulation Extrinsic muscle EMG	11.3 ± 2.1 (99)	21.3 ± 7.4 (45)

[a] Mean ± SD.
[b] Ketamine anesthesia.
[c] Number of cells.
[d] Number of responses in 200 trials recorded in four rats.

average values of the Δt_1 and Δt_2 latencies were similar for both muscle groups (Table 1). The slightly longer response latencies in vitro compared with those in vivo are consistent with the lower temperature of slice experiments and the lower conduction velocity of trigeminal sensory fibers in P12 to P15 versus adult animals (Cabanes et al., 2002).

To verify that the responses we recorded were not the result of direct electrical stimulation of the muscles, we unilaterally transected the facial nerve at the level of the buccolabialis junction, which lies upstream of the mystacial pad (Figure 3A). The lesion spared the branch of the VII-th nerve that innervated the levator labii superioris extrinsic muscle (e.g., Dörfl, 1982). In all animals (n = 5), this procedure suppressed the EMG responses in the intrinsic muscles (Figure 3C, upper panel). In contrast, transection did not abolish the EMG responses in the extrinsic muscle (Figure 3C, lower panel).

To complete the correspondence between in vivo and in vitro results for IoN stimulation, we investigated the dependence of the evoked EMG responses on the intensity and frequency of IoN stimulation. For purposes of quantification, we calculated the integrated response of the rectified EMG from the intrinsic muscles, denoted

$$\int dt\, |EMG_{Intrinsic}|,$$

where the integration limits extend over the ~5 ms duration of the Δt_1 or the Δt_2 response (Figure 3E, inset). We observed that an increase in stimulation current resulted in a nearly linear increase in the integrated EMG signal as an average across trials (n = 4) (Figure 3E).

With regard to the frequency of stimulation, both the intrinsic and extrinsic EMG amplitudes decreased as stimulation frequency increased (Figure 3F). Quantitatively, for a 200 ms interstimulus interval and either the Δt_1 or the Δt_2 response, the integrated EMG intrinsic and extrinsic responses after the second of two successive stimuli were 0.9 to 1 times that after the first (Table 2). This value decreased to ~0.4 for Δt_1 responses and ~0.2 for Δt_2 responses (Table 2). This trend is similar to that seen in vitro (Figure 1F), although the decrement is more pronounced in vivo.

Buccolabialis Stimulation

In the second method of sensory stimulation, the buccolabialis branch of the facial nerve was electrically excited (Figure 4A). Stimulation with currents two to three times that of the threshold for vibrissa protraction led to a large, compound muscle action potential with a latency of ~1 ms and a duration of ~3 ms (Figure 4B). In all animals (n = 7), the initial compound potential was followed by smaller, variable responses that resembled the EMGs seen upon IoN stimulation (cf. Figures 3D and 4D, upper panels). Further, the data for the EMG responses (4 rats and 200 trials) were separated into two groups, i.e., Δt_1 and Δt_2, as in the case of IoN stimulation. The mean latency for the group of Δt_1 responses elicited by facial nerve stimulation was 4–6 ms longer than that triggered by IoN stimulation (Table 1), consistent with the delay from motor nerve to IoN activation by muscle contraction (data not shown).

Stimulation of the facial nerve induced EMG responses in the vibrissa extrinsic muscles (Figures 4C and 4D, lower panels). To confirm that the EMG responses were driven by IoN sensory input rather than antidromic activation of vibrissa motoneurons, we transected the IoN in three rats. This manipulation abolished the delayed response induced by buccolabialis stimulation in all muscle groups of all animals (Figure 4C).

Passive Deflection

We ascertained whether the EMG responses observed upon simulated whisking (Figure 4) could be elicited solely by passive tactile stimulation of the vibrissae. We induced ~1° amplitude trains of rhythmic vibrissa motion at frequencies ranging from 2.5 Hz to 100 Hz (Figure 5A); each train was delivered at 3 s intervals and repeated 100 times. We observed EMG responses with variable amplitudes that followed the mechanical stimulus in the intrinsic muscles and in the levator labii extrinsic muscle (Figure 5B). Critically, the EMG re-

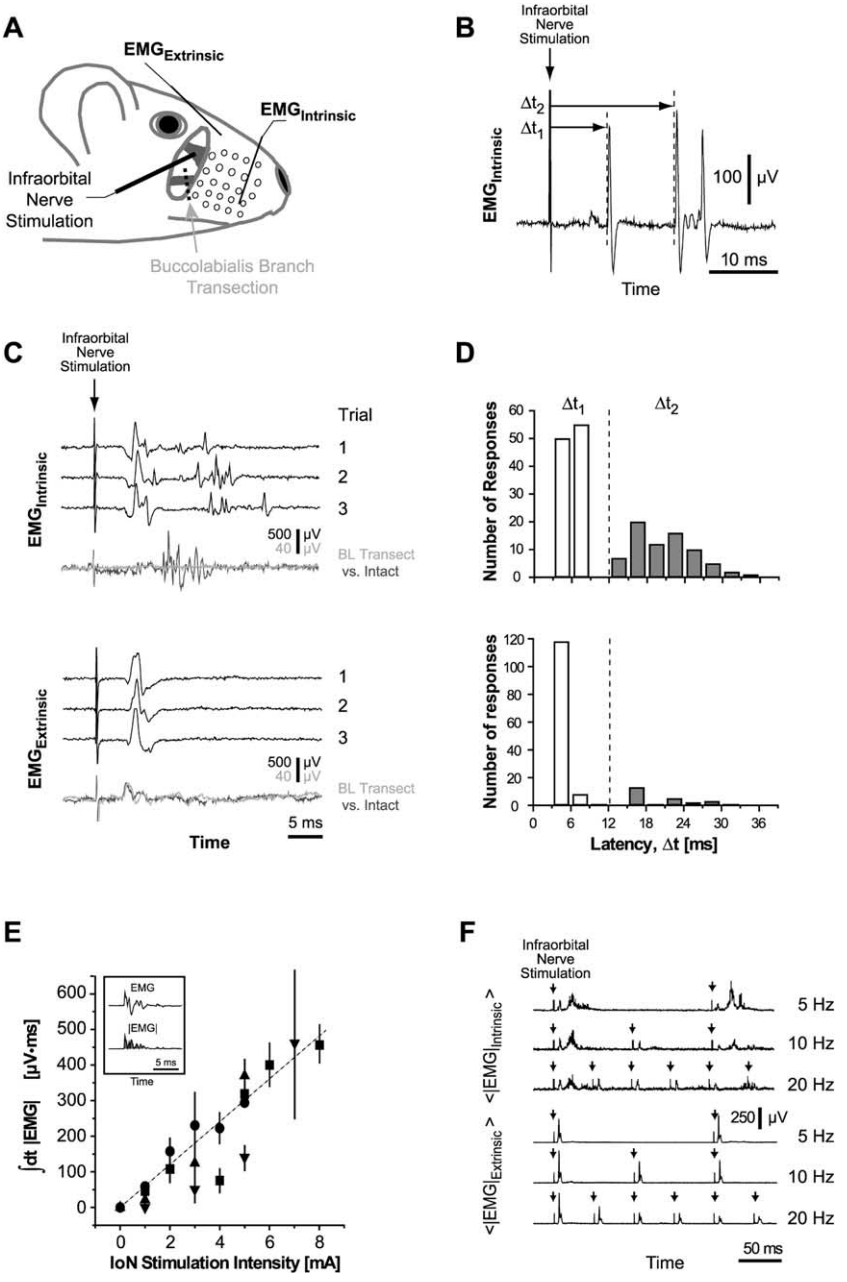

Figure 3. EMG Responses Elicited by Stimulation of the IoN in Ketamine-Xylazine Anesthetized Rats

(A) Experimental setup. (B) Response latencies Δt_1 and Δt_2 in a single trial. (C) Simultaneous recordings of EMG signals in ipsilateral intrinsic and extrinsic vibrissa muscles in three successive trials. The IoN was stimulated with a 5 mA, 200 μs current pulse delivered every 2 s. Average EMGs recorded before (light gray) and after (dark gray) transection of the buccolabialis branch are shown for a different rat. Traces are averages of 10 consecutive responses following IoN stimulation at 10 Hz with 8 mA, 100 μs pulses. (D) Distribution of response latencies in four rats (50 trials per rat). (E) Integral of rectified EMG responses of intrinsic muscles ($\int dt\,|EMG|$, inset, gray area in bottom trace) in four rats in response to increase in ION stimulation intensity (100 μs duration, delivered every 2 s). Each symbol represents a different animal. Each data point is the average (±SEM) of 10 to 20 trials; the line shows the trend. (F) Frequency-dependent depression of the averaged rectified trigeminally-evoked EMG response in intrinsic muscles and in the levator labii extrinsic muscle of the same rat. Each trace is the average of 20 rectified EMG records in response to repetitive IoN stimulations with 3 mA, 100 μs pulses. Arrows indicate IoN stimulation, which produces a stimulus artifact. Notice that the EMG responses consist of mixed Δt_1 and Δt_2 components in the intrinsic muscles and only a Δt_1 component in the extrinsic muscle.

sponses to passive vibrissa deflection were depressed after the first deflection for interstimulus intervals shorter than 200 ms (Figure 5B) (n = 5 rats). The distribution of latencies after the first deflection was similar to that of the Δt_2 responses recorded in the same rats during simulated whisking (Figure 5C). Lastly, the aver-

Table 2. Integrated EMG Paired-Pulse Responses after IoN Stimulation

	Interstimulus Interval 200 ms (5 Hz)[b]	Interstimulus Interval 100 ms (10 Hz)[b]
$\frac{\int_{\text{response}}^{\text{second } \Delta t_1} dt\ \lvert EMG\rvert}{\int_{\text{response}}^{\text{first } \Delta t_1} dt\ \lvert EMG\rvert}$ [a]	0.91 ± 0.12 (n = 3)[c]	0.40 ± 0.24 (n = 4)
$\frac{\int_{\text{response}}^{\text{second } \Delta t_2} dt\ \lvert EMG\rvert}{\int_{\text{response}}^{\text{first } \Delta t_2} dt\ \lvert EMG\rvert}$	0.96 ± 0.23 (n = 5)	0.19 ± 0.17 (n = 9)

[a] Average of both intrinsic and extrinsic muscle responses.
[b] Mean ± SD.
[c] 20 trials per rat.

age latencies for passive protraction (26.2 ± 6.8 ms; n = 75 events) and retraction (27.5 ± 6.2 ms; n = 104) in intrinsic muscles were statistically equivalent.

Simulated Whisking and Contact

We ascertained whether EMG responses could be elicited by contact of the vibrissae with an edge during simulated whisking, a requirement for physiological relevance of the positive feedback signal. The buccolabialis branch of the facial nerve was rhythmically excited to drive the vibrissa muscles at physiological whisking rates. The stimulation current was set at three times the threshold for vibrissa motion and consisted of a 5–20

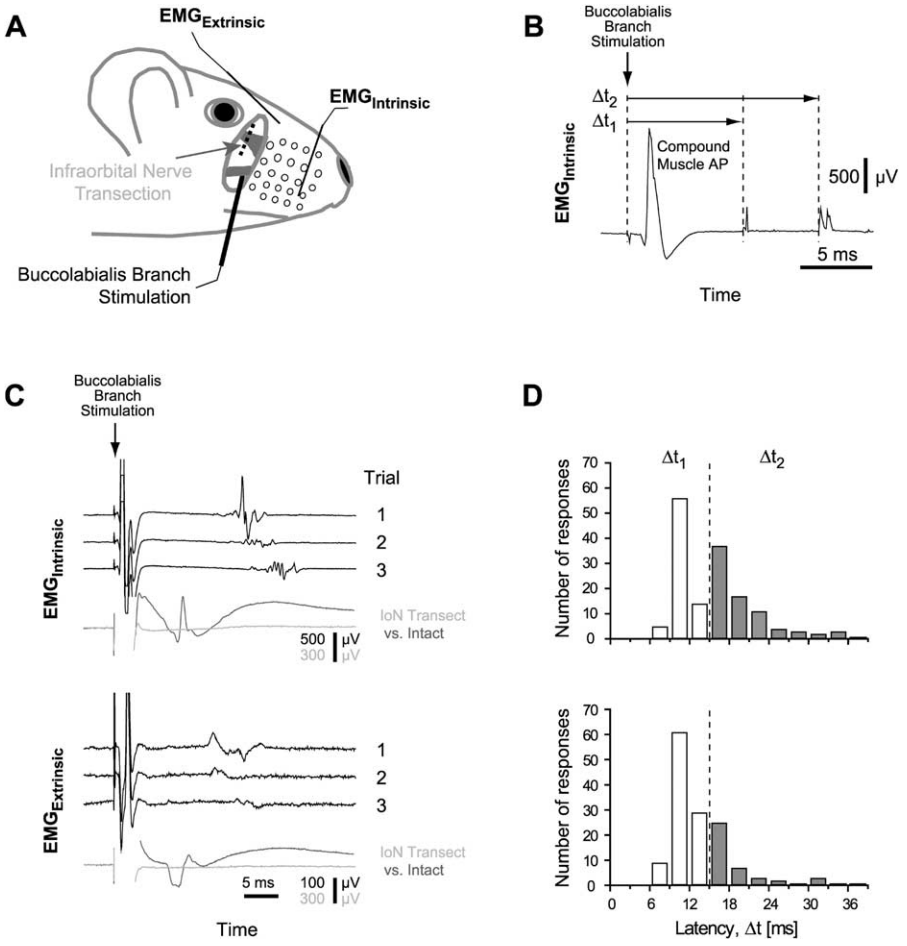

Figure 4. EMG Responses Elicited by Artificial Whisking in Ketamine-Xylazine Anesthetized Rats

(A) Experimental setup. (B) Response latencies Δt_1 and Δt_2 in a single trial. (C) Simultaneous recordings of EMG signals in ipsilateral intrinsic and extrinsic vibrissa muscles in three successive trials. The buccolabialis branch was stimulated with a 3 mA, 50 μs pulse delivered every 2 s. Average EMGs recorded before (light gray) and after (dark gray) transection of the infraorbital branch are shown for another rat. Traces are averages of 40 consecutive responses following buccolabialis stimulation at 0.5 Hz with 6 mA, 50 μs pulses. (D) Distribution of response latencies in four rats (50 trials per rat).

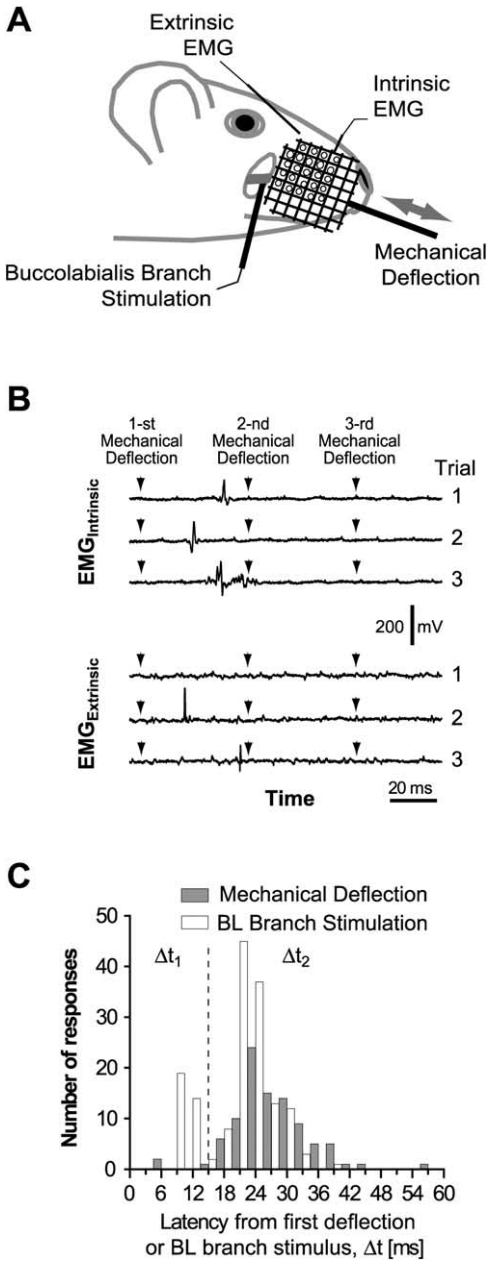

Figure 5. EMG Responses Elicited by Passive Vibrissa Deflection in Ketamine-Xylazine Anesthetized Rats

(A) Experimental setup for mechanical stimulation of the vibrissae. (B) EMG responses in intrinsic vibrissa muscles and in the levator labii superioris extrinsic muscle in response to a 20 Hz train of protractions in three consecutive trials. (C) Distribution of EMG response latencies in intrinsic muscles upon passive protraction (black bars) or simulated whisking through rhythmic stimulation of the buccolabialis branch of the facial nerve (gray bars) in five rats (100–116 trials per rat).

Hz train that was 0.5 s in duration and repeated every 2–3 s. A rigid contact detector was introduced in the trajectory of columns of vibrissae during alternating sets of trains (Figure 6A). Data shown here were collected for placements of the obstacle that maximized the EMG responses.

Placement of the obstacle along the vibrissa trajectory resulted in the transient increase in the rectified $EMG_{Intrinsic}$ (six of seven rats) and $EMG_{Extrinsic}$ (five of six rats) responses. Similar to the case of passive vibrissa stimulation (Figure 5), while the first contact in a train elicited an increase in the rectified $EMG_{Extrinsic}$ and $EMG_{Extrinsic}$ responses, the subsequent contacts had a negligible effect for stimulation frequencies above 5 Hz (Figure 6B); this was found in all animals tested (n = 7).

To quantify the amplitude of the contact-driven EMG response and establish the statistical significance of this effect, we formed distributions of the integral of rectified EMG responses for the intrinsic and in extrinsic muscles. Each datum consisted of the integrated response,

$$\int_{\text{response}}^{\text{first } \Delta t_2} dt\, |EMG_{Intrinsic}|$$

or

$$\int_{\text{response}}^{\text{first } \Delta t_2} dt\, |EMG_{Extrinsic}|,$$

after the first stimulation for both contact and noncontact cases (Figure 6C). The distributions when the obstacle was present were significantly different from those when the obstacle was removed, as judged by a Kolmogorov-Smirnov test on the cumulatives (Figure 6C, insets). Overall, the presence of the obstacle increased the area of the rectified EMG responses for the intrinsic muscles by 129 ± 109% (n = 7 rats) (Figure 6D). Similarly, in the extrinsic muscle levator labii superioris, contact increased the area of rectified EMG responses by 202 ± 64% (n = 6) (Figure 6D).

Discussion

We have demonstrated, based on in vitro (Figures 1 and 2) and in vivo (Figures 3–6) approaches, that the vibrissa trigeminal loop (Figure 1A) is an excitatory reflex arc. Activation of the intrinsic vibrissa muscles triggers a sensory-mediated increase in the drive to both the intrinsic and extrinsic vibrissa muscles (Figure 4). Further, both passive movement of the vibrissae (Figure 5) and active touch of the vibrissae against an obstacle (Figure 6) lead to an increase in the drive to both the intrinsic and extrinsic vibrissa muscles. This increase is rapidly depressed for contact at 100 ms intervals, which corresponds to the ~10 Hz center frequency for exploratory whisking (see Nguyen et al., 2004 for a compendium of frequencies). Our conclusion that the vibrissa trigeminal loop is an excitatory reflex arc is corroborated by prior results obtained in awake, behaving rats. In particular, cutting the IoN reduces mean whisking frequencies by ~25% (Berg and Kleinfeld, 2003; Welker, 1964). Further, passive vibrissa deflection induces an EMG signal in vibrissa muscles (Kleinfeld et al., 2002). Lastly, an increase in the amplitude of the mystacial EMG is detected when rats touch objects with their vibrissae (Sachdev et al., 2003).

The initial motoneuron or EMG response that follows IoN stimulation has a very short latency, i.e., Δt_1 of 5–10 ms, and is likely to be mediated by direct connections

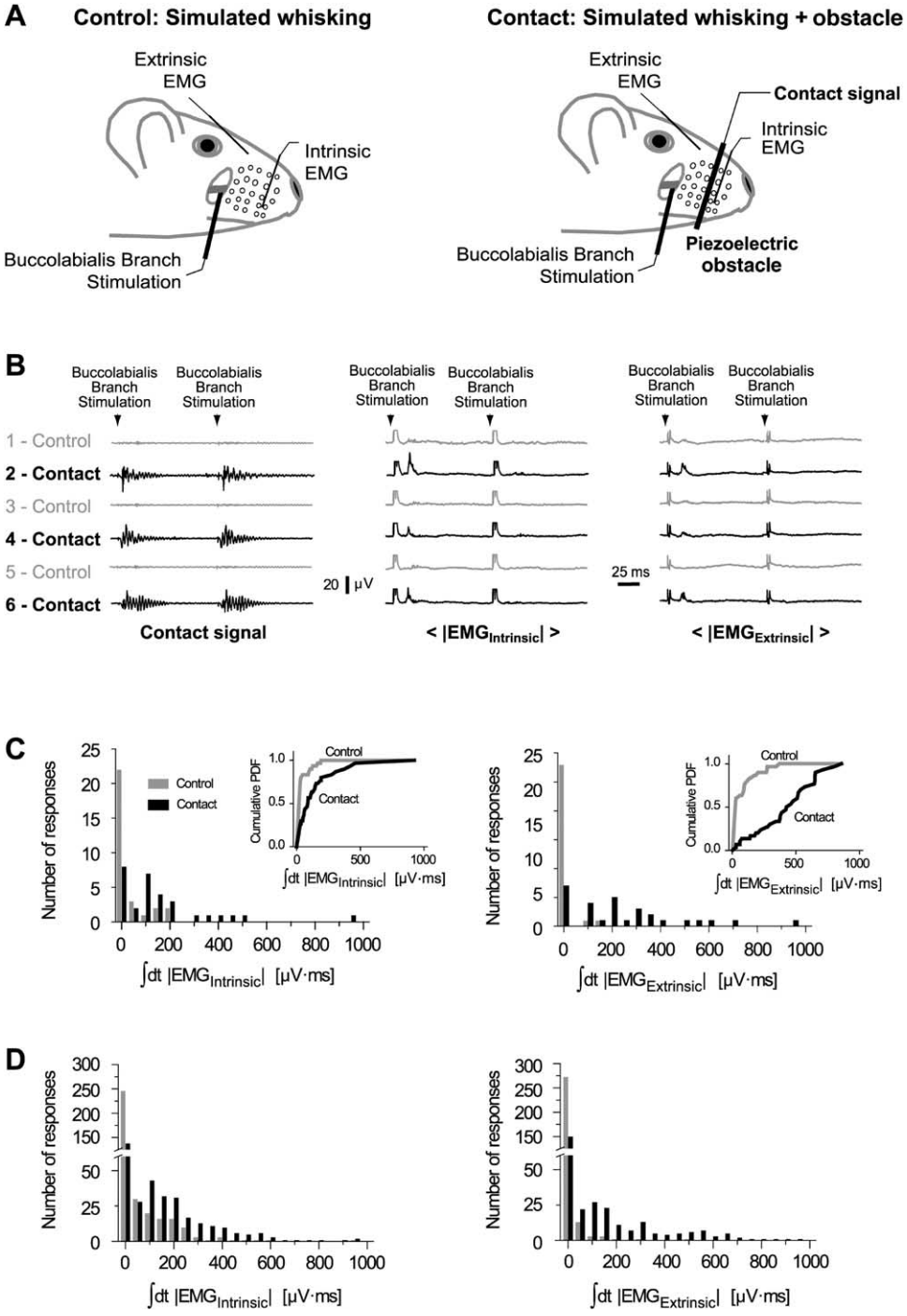

Figure 6. EMG Responses Elicited by Vibrissa Contact in Ketamine-Xylazine Anesthetized Rats

(A) Experimental setup for contact experiment during simulated whisking. (B) Contact signal (left traces) and consecutive averaged rectified EMG responses recorded simultaneously in intrinsic (middle traces) and extrinsic (right traces) vibrissa muscles. Each trace is the average of 30 sweeps, obtained by stimulating the buccolabialis branch of the facial nerve at 8 Hz with 9 mA, 50 μs pulses. In the <|$EMG_{intrinsic}$|> records, the initial compound muscle action potential (e.g., Figure 4B) was truncated for the sake of clarity. (C) Distribution of the integral of the rectified EMG response in intrinsic (left graph) and levator labii superioris extrinsic (right graph) muscles during simulated whisking with (gray bars) or without contact (black bars) in one rat. The inset in each graph is a plot of the cumulated probability density function of the integral of the rectified EMG response in the presence or the absence of contact. (D) Distribution of the integral of the rectified EMG response in intrinsic (left graph; n = 7 rats) and extrinsic (right graph; n = 6 rats) muscles during simulated whisking with (gray bars) or without contact (black bars).

between the trigeminal sensory nuclei and the facial nucleus. The longer latency response, i.e., Δt_2 of ~25 ms, is most probably created by the activation of indirect trigeminofacial connections, since longer pathways, such as the loops involving the superior colliculus (Kleinfeld et al., 1999), are absent from the in vitro preparation. We postulate that the longer latency response in vivo is mediated by indirect trigeminofacial connections that involve the reticular formation (Dauvergne et al., 2001; Zerari-Mailly et al., 2001) or by local connections within the trigeminal sensory complex (Jacquin et al., 1990).

Active touch requires tapping or probing the edges and surfaces of an object. We speculate that excitatory sensorimotor feedback to vibrissa muscles may act to hold tactile sensors on the surface of the object to be probed (Gibson, 1962) and thus increase the reliability of a contact-dependent sensory signal. Further, texture discrimination is likely to depend on the force and speed imparted to the sensors (Carvell and Simons, 1995; Hartmann et al., 2003; Mehta and Kleinfeld, 2004; Neimark et al., 2003). We speculate that positive sensory feedback in the vibrissa trigeminal loop optimizes these parameters.

Sufficiently strong and prolonged positive feedback could, in principle, allow minor disturbances of the vibrissae to develop into full rhythmic whisks. Yet this appears not to be the case (Kleinfeld et al., 2002). Nor does positive feedback provide the mechanism for rhythmic whisking, as multiple studies have found that exploratory whisking occurs after the IoN is lesioned (Berg and Kleinfeld, 2003; Gao et al., 2001; Welker, 1964). Our results suggest that depression of the sensory-induced EMG response, as seen in vivo (Figures 3F and 5B), could account for the lack of reverberating activity in the vibrissa trigeminofacial loop. The onset of depression is strong near the 10 Hz frequency of exploratory whisking (Berg and Kleinfeld, 2003; Welker, 1964), but weak at low frequencies (Figures 3F and 5B and Table 2). The more rapid depression of the in vivo EMG response with increasing frequency compared with that of the in vitro EPSP response (Figure 1F) is consistent with a threshold nonlinearity in the conversion of EPSPs to action potentials.

The eyeblink reflex circuit and the vibrissa sensorimotor loop share a common anatomy. The eyeblink reflex, which can be elicited by stimulating the supraorbital branch of the trigeminal nerve, activates the orbicularis oculi muscle via trigeminal connections to the facial nerve and leads to eyelid closure (Holstege et al., 1995). The eyeblink reflex is characterized by two EMG responses in orbicularis oculi (Dumitru, 1995), whose time courses parallel those observed for the vibrissa system (Δt_1 and Δt_2 in Figure 2). In the human disease blepharospasm (Hallett, 2002), the blink circuit is overactive, possibly because of striatal dopaminergic depletion (Schicatano et al., 1997). Interestingly, unintentional whisking is observed in rats upon the administration of apomorphine (e.g., Filipkowski et al., 2001), a D2 dopaminergic receptor antagonist. We thus conjecture that: (1) eyeblink shares a common physiology, in addition to a common anatomy, with the vibrissa trigeminal loop; and (2) involuntary blink oscillations, the cardinal sign of blepharospasm, are caused by an abnormally high sensory positive feedback. This speculation is buttressed by the observation that the onset of depressed EMG responses from paired pulse stimulation of the trigeminal nerve occurs at higher frequencies in patients with blepharospasm than in normal subjects (Aramideh and Ongerboer de Visser, 2002).

Experimental Procedures

Brainstem Slice Preparation

Sprague Dawley rats, aged P7 to P15, were deeply anesthetized with halothane and then decapitated. The cranium was opened and quickly immersed in an ice-cold cutting solution (220 mM sucrose, 2.5 mM KCl, 3 mM $MgSO_4$, 26 mM $NaHCO_3$, 1.25 mM NaH_2PO_4, 1 mM $CaCl_2$, and 10 mM D-glucose, 7 mM $MgCl_2$, and 4 mM lactic acid) bubbled with carbogen (95% O_2 and 5 %CO_2) for final pH values of 7.35–7.40. The forebrain was cut transversally at the level of the temporal cortex and discarded. In P12 to P15 animals, the trigeminal nerves were carefully dissected down to the trigeminal ganglion. In younger animals, the trigeminal nerve was further dissected to include the infraorbital branch of the nerve (IoN) down to the vibrissa pad. Isolation of IoN was done only in P7 to P9 rats, because in older animals, IoN dissection was too time-consuming to ensure healthy slices. After removing the cerebellum and the tectum, the brainstem block was glued dorsal side down onto a slanted edge mounted on a cutting dish and then placed on a vibrating microtome (Vibratome 1000; TPI Inc., CA). A first cut removed the pyramidal and rubrospinal tracts, exposing the lateral subdivision of the facial nucleus. After the blade was lowered by 1000–1200 μm, a second cut separated the slice. In preparations from newborn animals, we were able to surgically isolate the infraorbital branch of the trigeminal nerve (IoN) down to the vibrissa pad while neurons in the slice remained viable. All aspects of experimental manipulation were in strict accordance with guidelines from the National Institutes of Health and were approved by the University of California at San Diego Institutional Animal Care and Use Committee.

Location of Vibrissa Motoneurons

The presence of vibrissa motoneurons in the slice was confirmed by retrograde transport of the fluorescent dye Evans Blue. Two to three days prior to dissection, a volume of 20–30 μl of 2% (w/v) Evans Blue in phosphate-buffered saline was injected in each mystacial pad. Retrogradely labeled neurons were imaged with a confocal microscope (MRC-1024, BioRad, CA) using a 568 nm excitation wavelength and a 585 nm long-pass emission filter. The tracer also labeled the trigeminal nerves, in which staining was observed prominently in fibers inside the spinal trigeminal tract (Figure 1B). Consistent with past work (Cajal, 1909), no labeled trigeminal processes could be seen entering the facial nucleus.

Vibrissa Motoneuron Recording

The slice was placed in the recording chamber filled with artificial ACSF (126 mM NaCl, 5 mM KCl, 2 mM $MgSO_4$, 26 mM $NaHCO_3$, 1.25 mM NaH_2PO_4, 2 mM $CaCl_2$, and 10 mM D-glucose bubbled with carbogen) and set at 32°C. The IoNs (P7 to P9) or the entire trigeminal nerves (P12 to P15) were inserted into suction electrodes connected to an extracellular isolated voltage stimulator (DS2A; Digitimer, UK). Stimuli consisted of monopolar voltage pulses, 200 μs each at a frequency of 0.5 Hz or higher, through the suction electrode. Membrane potentials were recorded using sharp electrodes filled with 1.5 M potassium acetate (25–80 MΩ). The viability of the preparation was assayed through the characterization of the motoneurons (Aghajanian and Rasmussen, 1989; Nguyen et al., 2004). These cells had a resting potential of –63 ± 6 mV (n = 24) and –62 ± 7 mV (n = 75) for P7 to P9 and P11 to P15 animals, respectively; had an input resistance of 30 ± 12 MΩ across both age groups; and fired regenerative spikes upon current injection. The motoneurons remained suitable for recording for up to 6 hr in these thick slices. Response latencies were always measured as

the time from the trigeminal stimulation to the onset of the first EPSP.

In Vivo Electromyogram Recordings

Vibrissa muscle-evoked EMG responses were recorded in adult Sprague Dawley rats (230–275 g). Animals were anesthetized with intraperitoneal injections of either urethane (1.2 g/kg body weight) or ketamine (50 mg/kg) and xylazine (10 mg/kg); for the latter group, half-doses of ketamine-xylazine were administered every 30–45 min. The infraorbital branch of the trigeminal nerve was exposed on one side by making a dorsoventral incision caudal to the mystacial pad and anteroventral to the eye. Care was taken to spare extrinsic muscles overlying the infraorbital branch. The facial nerve was exposed at the level of the junction between the buccal and upper marginal mandibular branches before they enter the mystacial pad. The trigeminal and facial nerves were excited at frequencies ranging from 0.5–50 Hz with 50– 200 μs monopolar current pulses delivered by an isolated stimulator (Isolator-11, Axon Instruments, CA). The stimulator output was connected to a 1 mm diameter concentric bipolar electrode (FHC Corp., ME) directly positioned onto nerves and adjusted to maximize the EMG response. Neither trigeminal nor facial nerve stimulations induced contraction of muscles surrounding the electrode or spurious reflexes such as eye blinking. To place recording electrodes, the skin was incised over the recording sites, and two to three tungsten electrodes fashioned from 0.005 inch Micro-Probes (A-M Systems, WA) were placed rostrally, caudally, and often medially in the mystacial pad, while a similar electrode was inserted in the ipsilateral levator labii superioris extrinsic muscle (Berg and Kleinfeld, 2003). The reference electrode was placed in the midline of the snout. Muscle action potentials were amplified 200 to 6400 times and band-pass filtered between 2 Hz and 10 kHz before being digitized. Response latencies were always measured as the time from the trigeminal stimulation to the onset of the first EMG response during the Δt_1 window (0–12 ms) or the Δt_2 window ($\geq$12 ms). Transections were performed with iridectomy scissors in experiments that involved the lesion of the IoN branch of the Vth nerve or the buccolabialis branch of the VII-th nerve. In passive deflection experiments, vibrissae were held by a nylon mesh attached to a piezoelectric-based actuator (Ahrens et al., 2002). In contact experiments, vibrissae were made to touch a piezoelectric rigid film, which was used both as an obstacle to vibrissa motion and as a contact detector. During contact experiments, the level of anesthesia was maintained by regular injections of small doses of ketamine-xylazine (50 mg/kg and 5 mg/kg for ketamine and xylazine, respectively) every 8–10 min.

Acknowledgments

We thank M. Brecht, C. Evinger, D. Golomb, A. Keller, H. P. Killackey, and F.-S. Lo for pertinent discussions and B. Friedman and S.B. Mehta for comments on earlier versions of the manuscript. Supported by the NIH (grant MH59867) and the Human Science Frontiers program.

Received: June 4, 2004
Revised: October 1, 2004
Accepted: December 3, 2004
Published: February 2, 2005

References

Aghajanian, G.K., and Rasmussen, K. (1989). Intracellular studies in the facial nucleus illustrating a simple new method for obtaining viable motoneurons in adult rat brain slices. Synapse *3*, 331–338.

Ahrens, K.F., Levine, H., Suhl, H., and Kleinfeld, D. (2002). Spectral mixing of rhythmic neuronal signals in sensory cortex. Proc. Natl. Acad. Sci. USA *99*, 15176–15181.

Aramideh, M., and Ongerboer de Visser, B.W. (2002). Brainstem reflexes: electrodiagnostic techniques, physiology, normative data, and clinical applications. Muscle Nerve *26*, 14–30.

Berg, R.W., and Kleinfeld, D. (2003). Rhythmic whisking by rat: Retraction as well as protraction of the vibrissae is under active muscular control. J. Neurophysiol. *89*, 104–117.

Brown, A.W.S., and Waite, P.M.E. (1974). Responses in the rat thalamus to whisker movements produced by motor nerve stimulation. J. Physiol. *238*, 387–401.

Cabanes, C., Lopez de Armentia, M., Viana, F., and Belmonte, C. (2002). Postnatal changes in membrane properties of mice trigeminal ganglion neurons. J. Neurophysiol. *87*, 2398–2407.

Cajal, S.R. (1909). Histologie du Système Nerveux de l'Homme et des Vertébrés (Paris: Maloine).

Carvell, G.E., and Simons, D.J. (1995). Task-and subject-related differences in sensorimotor behavior during active touch. Somatosens. Mot. Res. *12*, 1–9.

Dauvergne, C., Pinganaud, G., Buisseret, P., Buisseret-Delmas, C., and Zerari-Mailly, F. (2001). Reticular premotor neurons projecting to both facial and hypoglossal nuclei receive trigeminal afferents in rats. Neurosci. Lett. *311*, 109–112.

Dörfl, J. (1982). The musculature of the mystacial vibrissae of the white mouse. J. Anat. *135*, 147–154.

Dumitru, D. (1995). Electrodiagnostic Medicine (Philadelphia: Hanley and Belfus).

Erzurumlu, R.S., and Killackey, H.P. (1979). Efferent connections of the brainstem trigeminal complex with the facial nucleus of the rat. J. Comp. Neurol. *188*, 75–86.

Evinger, C., Basso, M.A., Manning, K.A., Sibony, P.A., Pellegrini, J.J., and Horn, A.K. (1993). A role for the basal ganglia in nicotinic modulation of the blink reflex. Exp. Brain Res. *92*, 507–515.

Fanselow, E.E., and Nicolelis, M.A.L. (1999). Behavioral modulation of tactile responses in the rat somatosensory system. J. Neurosci. *19*, 7603–7616.

Filipkowski, R.K., Rydz, M., and Kaczmarek, L. (2001). Expression of c-Fos, Fos B, Jun B, and Zif268 transcription factor proteins in rat barrel cortex following apomorphine-evoked whisking behavior. Neuroscience *106*, 679–688.

Friauf, E. (1986). Morphology of motoneurons in different subdivisions of the rat facial nucleus stained intracellularly with horseradish peroxidase. J. Comp. Neurol. *253*, 231–241.

Gamzu, E., and Ahissar, E. (2001). Importance of temporal cues for tactile spatial-frequency discrimination. J. Neurosci. *21*, 7416–7427.

Gao, P., Bermejo, R., and Zeigler, H.P. (2001). Vibrissa deafferentation and rodent whisking patterns: behavioral evidence for a central pattern generator. J. Neurosci. *21*, 5374–5380.

Gibson, J.J. (1962). Observations on active touch. Psychol. Rev. *69*, 477–491.

Guido, W., Lo, F.S., and Erzurumlu, R.S. (2001). Synaptic plasticity in the trigeminal principal nucleus during the period of barrelette formation and consolidation. Brain Res. Dev. Brain Res. *132*, 97–102.

Hallett, M.H. (2002). Blepharospasm: recent advances. Neurology *59*, 1306–1312.

Hartmann, M.J., Johnson, N.J., Towal, R.B., and Assad, C. (2003). Mechanical characteristics of rat vibrissae: resonant frequencies and damping in isolated whiskers and in the awake behaving animal. J. Neurosci. *23*, 6510–6519.

Hattox, A.M., Priest, C.A., and Keller, A. (2002). Functional circuitry involved in the regulation of whisker movements. J. Comp. Neurol. *442*, 266–276.

Hattox, A.M., Li, Y., and Keller, A. (2003). Serotonin regulates rhythmic whisking. Neuron *39*, 343–352.

Holstege, G., Blok, B.F.M., and ter Horst, G.J. (1995). Brainstem systems involved in the blink reflex, feeding mechanisms, and micturition. In The Rat Nervous System, G. Paxinos, ed. (San Diego: Academic Press), pp. 257–275.

Jacquin, M.F., Chiaia, N.L., Haring, J.H., and Rhoades, R.W. (1990). Intersubnuclear connections within the rat trigeminal brainstem complex. Somatosens. Mot. Res. *7*, 399–420.

Kis, Z., Rakos, G., Farkas, T., Horvath, S., and Toldi, J. (2004). Facial nerve injury induces facilitation of responses in both trigeminal and facial nuclei of rat. Neurosci. Lett. *358*, 223–225.

Kleinfeld, D., Berg, R.W., and O'Connor, S.M. (1999). Anatomical loops and their electrical dynamics in relation to whisking by rat. Somatosens. Mot. Res. *16*, 69–88.

Kleinfeld, D., Sachdev, R.N.S., Merchant, L.M., Jsarvis, M.R., and Ebner, F.F. (2002). Adaptive filtering of vibrissa input in motor cortex of rat. Neuron *34*, 1021–1034.

Li, Y.-Q., Takada, M., Kaneko, T., and Mizuno, N. (1997). Distribution of GABAergic and glycinergic premotor neurons projecting to the facial and hypoglossal nuclei in the rat. J. Comp. Neurol. *378*, 283–294.

Llinás, R., and Yarom, Y. (1981). Electrophysiology of mammalian inferior olivary neurones in vitro. Different types of voltage-dependent ionic conductances. J. Physiol. *315*, 549–567.

Lo, F.S., Guido, W., and Erzurumlu, R.S. (1999). Electrophysiological properties and synaptic responses of cells in the trigeminal principal sensory nucleus of postnatal rats. J. Neurophysiol. *82*, 2765–2775.

Mehta, S.B., and Kleinfeld, D. (2004). Frisking the whiskers: patterned sensory input in the rat vibrissa system. Neuron *41*, 181–184.

Minnery, B.S., and Simons, D.J. (2003). Response properties of whisker-associated trigeminothalamic neurons in rat nucleus principalis. J. Neurophysiol. *89*, 40–56.

Neimark, M.A., Andermann, M.L., Hopfield, J.J., and Moore, C.I. (2003). Vibrissa resonance as a transduction mechanism for tactile encoding. J. Neurosci. *23*, 6499–6509.

Nguyen, Q.-T., Wessel, R., and Kleinfeld, D. (2004). Developmental regulation of active and passive membrane properties in rat vibrissa motoneurones. J. Physiol. *556*, 203–219.

Onodera, K., Hamba, M., and Takahashi, T. (2000). Primary afferent synaptic responses recorded from trigeminal caudal neurons in a mandibular nerve-brainstem preparation of neonatal rats. J. Physiol. *524*, 503–512.

Rice, F.L., Fundin, B.T., Arvidsson, J., Aldskogius, H., and Johansson, O. (1997). Comprehensive immunofluorescence and lectin binding analysis of vibrissal follicle sinus complex innervation in the mystacial pad of the rat. J. Comp. Neurol. *385*, 149–184.

Sachdev, R.H.S., Berg, R.W., Chompney, G., Kleinfeld, D., and Ebner, F.F. (2003). Unilateral vibrissa contact: Changes in amplitude but not the timing of vibrissa movement. Somatosens. Mot. Res. *20*, 162–169.

Schicatano, E.J., Basso, M.A., and Evinger, C. (1997). Animal model explains the origins of the cranial dystonia benign essential blepharospasm. J. Neurophysiol. *77*, 2842–2846.

Sosnik, R., Haidarliu, S., and Ahissar, E. (2001). Temporal frequency of whisker movement. I. Representations in brain stem and thalamus. J. Neurophysiol. *86*, 339–353.

Szwed, M., Bagdasarian, K., and Ahissar, E. (2003). Coding of vibrissal active touch. Neuron *40*, 621–630.

Voisin, J., Lamarre, Y., and Chapman, C.E. (2002). Haptic discrimination of object shape in humans: contribution of cutaneous and proprioceptive inputs. Exp. Brain Res. *145*, 251–260.

Welker, W.I. (1964). Analysis of sniffing of the albino rat. Behaviour *12*, 223–244.

Wineski, L.E. (1983). Movements of the cranial vibrissae in the golden hamster (Mesocritus auratus). J. Zool. *200*, 261–280.

Zerari-Mailly, F., Pinganaud, G., Dauvergne, C., Buisseret, P., and Buisseret-Delmas, C.J. (2001). Trigemino-reticulo-facial and trigemino-reticulo-hypoglossal pathways in the rat. J. Comp. Neurol. *429*, 80–93.

Zucker, E., and Welker, W.I. (1969). Coding of somatic sensory input by vibrissae neurons in the rat's trigeminal ganglion. Brain Res. *12*, 134–156.